Characteristics analysis of shock wave near nozzle in ejector

Mingyang He, Wei Lu*, Zhizhou Xu, and Penghao Xing

College of Mechanical Engineering, Guangxi University, 530004 Nanning, China

* Corresponding author: tjluwei@163.com

Abstract. With increasing concern of environmental and energy issues, ejector is more and more widely applied in various fields owing to the advantages of using low grade heat. In the ejector, the Mach waves may be generated at the nozzle outlet and diffuser chamber. Under different expansion ratios, the Mach waves at the nozzle outlet will appear to be expansion waves, oblique shock waves and normal shock waves successively. This paper theoretically studies the characteristics of the Mach waves at the nozzle exit of the ejector with steam, ammonia, R22, R290, R134a and R600a as working fluids. The results indicate that the higher the adiabatic indexes, the lower the Mach wave intensity if there are oblique shock waves or expansion waves in the nozzle exit and; the cross section ratio and shock wave intensity vary gently with the rise of expansion ratio. At the same time, expansion wave intensity and shock wave intensity also decrease with the increase of nozzle cone angle. Therefore, there should be an optimal parametric range for nozzle structure design to obtain higher efficiency.

1. Introduction

Ejector is a fluid pressure rise device which can be driven by low-grade energy such as solar energy or exhausted energy. The supersonic working flow is obtained by using the larval nozzle to absorb and mix the low-pressure section flow[1-2]. Because of its simple-structure, reliability, and low-cost, it is widely used in process industries such as petrochemical, metallurgical engineering, vacuum, refrigeration and other energy industrial fields. In order to further enhance the environmental performance of jet refrigeration, more and more natural working fluid are used in this kind of refrigeration system[3-5].

The structure of the ejector with flow regime and the internal mach waves is showed in Fig.1. The ejector comprises of a laval nozzle, a suction chamber, mixing chamber and diffuser. High pressure refrigerant, known as the primary fluid, is accelerated through the laval nozzle and converted into high speed flow with low pressure[6]. The secondary flow is entrained into the ejector from the suction chamber. The flow direction from the outlet of the power nozzle can be divided into two states: drive flow regime and suction flow regime. On the shear layer of the driving flow boundary, part of kinetic energy of the primary flow is transferred to the secondary flow. The two flows will eventually mix in the mixing chamber and jet out of the ejector. The pressure change of the nozzle outlet is described by the parameters E (expansion ratio), as shown in Eq.1.

$$E = P_b / P^* \qquad (1)$$

Where P_b is the pressure of secondary flow in the section chamber and P^* is total pressure of primary flow.

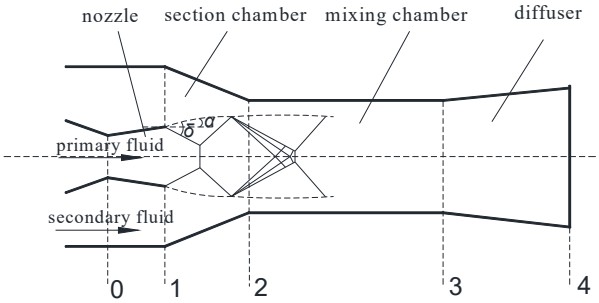

Fig. 1. The structure of the ejector.

In Fig.1, A_0 and A_e represent the cross-sectional area at the nozzle throat and outlet respectively. There are two positions inside of the ejector where mach waves may occur. At the position, mach waves can be expressed as expansion waves or shock waves. The driving flow mach waves may appear at the outlet of the nozzle, and the mixed flow shock wave may appear in the diffuser, where the mixed flow changes to subsonic speed from subsonic[7]. The shape of the mach waves at the outlet of nozzle based on the expansion ratio. There will be three conditions mach waves at the nozzle outlet, with the increase of expansion ratio, there appears expansion waves, oblique shock waves and straight shock wave successively.

2. Analysis model for ejector nozzle performance

In the one-dimensional theoretical model, the primary flow development is assumed as isentropic process in the nozzle. Known to the nozzle exit A_1/A_0, nozzle export work cone angle α, the pressure of secondary flow and total pressure of working flow for P_b/P^*, steam of adiabatic index k, depending on the backpressure ratio and the exit flow state can be divided into several ways.

The flow function $q(Ma)$ of nozzle outlet can be determined by the area ratio of nozzle outlet section.

$$q(Ma_1) = A_0 / A_1 \tag{2}$$

From the following equation, the mach numbers corresponding to the section ratio of the sub-sonic and supersonic sections of the nozzle can be obtained: Ma_{e1} and Ma_{e2}.

$$q(Ma) = Ma\left[\frac{2}{k+1}\left(1+\frac{k-1}{2}Ma^2\right)\right]^{-\frac{k+1}{2(k-1)}} \tag{3}$$

By type pneumatic function can be obtained under Π (Ma_{e1}), Π (Ma_{e2}) and the nozzle exit section on supersonic airflow pressure P_e.

$$\frac{P_e}{P^*} = \Pi(Ma) = \left(1+\frac{k-1}{2}Ma^2\right)^{-\frac{k}{k-1}} \tag{4}$$

The pressure ratio before and after shock wave was obtained by Ma_{e2}.

$$\frac{P_2}{P_1} = \frac{2k}{k+1}Ma_{e2}{}^2 - \frac{k-1}{k+1} \tag{5}$$

The three critical pressure strength ratios of nozzle outlet flow are obtained.

$$\begin{aligned}\left(\frac{P_b}{P^*}\right)_1 &= \Pi(Ma_{e2});\\ \left(\frac{P_b}{P^*}\right)_2 &= \frac{P_2}{P_1}\Pi(Ma_{e2});\\ \left(\frac{P_b}{P^*}\right)_3 &= \Pi(Ma_{e1})\end{aligned} \tag{6}$$

When $(P_b/P^*)_2<E<(P_b/P^*)_3$, straight shock waves will appear in the nozzle expansion section. The following equation is obtained by applying the continuity equation to the nozzle throat section and outlet section.

$$y(\lambda_e)=\frac{P^*}{P_b}\cdot\frac{A_0}{A_1} \tag{7}$$

The supersonic solutions λ_e and $q(\lambda_e)$ are shown in the following formula.

$$y(\lambda_e)=\frac{q(\lambda)}{\pi(\lambda)}=\lambda\cdot\left(\frac{k+1}{2}\right)^{\frac{1}{k+1}}\Bigg/\left(1-\frac{k-1}{k+1}\lambda^2\right) \tag{8}$$

$$q(\lambda_e)=\left(\frac{k+1}{2}\right)^{\frac{1}{k-1}}\cdot\lambda\cdot\left(1-\frac{k-1}{k+1}\lambda^2\right)^{\frac{1}{k-1}} \tag{9}$$

The total pressure ratio before and after shock wave is obtained by using the first continuity equation for nozzle throat and outlet.

$$\frac{P_{s2}^*}{P_{s1}^*}=\frac{P_e^*}{P_0^*}=\frac{A_0}{A_1}\cdot\frac{1}{q(\lambda_e)} \tag{10}$$

The Mach number before shock wave can be obtained by Eq.11

$$\frac{P_{s2}^*}{P_{s1}^*}=\left\{\left[\frac{k-1}{k+1}+\frac{2}{(k+1)Ma_{s1}^2}\right]^k\left(\frac{2k}{k+1}Ma_{s1}^2-\frac{k-1}{k+1}\right)\right\}^{\frac{1}{k-1}} \tag{11}$$

Connecting Eq.3 and continuity equation, get the shock cross section ratio

$$A_0/A_s=q(Ma_{s1}) \tag{12}$$

The straight shock wave intensity is

$$\beta=\frac{P_{s2}}{P_{s1}}=\frac{2k}{k+1}Ma_{s1}^2-\frac{k-1}{k+1} \tag{13}$$

When $(P_b/P^*)_3<E<(P_b/P^*)_2$, oblique shock waves will appear at the nozzle outlet and the mach number of the primary flow $Ma_{s1}=Ma_{e2}$, shock wave section ratio $A_s/A_0=A_1/A_0$. The strong and weak oblique shock wave angle δ_1, δ_2 is obtained by Eq.14.

$$\tan\alpha = \frac{Ma_1^2 \sin^2\delta - 1}{\left[Ma_1^2\left(\frac{k+1}{2}\right) - \sin^2\delta + 1\right]\tan\delta} \tag{14}$$

The mach number after oblique shock wave is

$$Ma_2^2 = \frac{Ma_1^2 + 2/k\text{-}1}{(2k/k\text{-}1)Ma_1^2\sin^2 d\text{-}1} + \frac{Ma_1^2\cos^2 d}{(k\text{-}1/2)Ma_1^2\sin^2 d + 1} \tag{15}$$

Total pressure ratio before and after oblique shock wave is

$$\frac{P_{s2}^*}{P_{s2}^*} = \left\{\left[\frac{2+(k\text{-}1)Ma_{s1}^2\sin^2\delta}{(k+1)Ma_{s1}^2\sin^2\delta}\right]^{-k}\left(\frac{2k}{k+1}Ma_{s1}^2\sin^2\delta\text{-}\frac{k\text{-}1}{k+1}\right)\right\}^{\frac{1}{k-1}} \tag{16}$$

The intensity of the oblique shock wave is

$$\beta = \frac{p_{s2}}{p_{s1}} = \frac{2k}{k+1}Ma_{s1}^2\sin\delta - \frac{k-1}{k+1} \tag{17}$$

When $E<(P_b/P^*)_3$, a series of expansion waves will appear at the nozzle outlet, mach number of primary flow before shock wave $Ma_{s1}=Ma_{e2}$, shock section ratio $As/A_0=A_1/A_0$. Assuming that the cone angle of the nozzle outlet section is the same, for the expansion wave, the left extension wave system and the right extension wave system only have different directions, take the cone angle α counterclockwise, and α is determined by Prandtl-Meyer function.

$$\alpha = \nu(Ma_{s2}) - \nu(Ma_{s1}) \tag{18}$$

Where, Ma_{s2} is solved by the following Eq.19.

$$\nu(Ma) = \sqrt{\frac{k+1}{k-1}}\arctan\sqrt{\frac{k-1}{k+1}\left(Ma^2-1\right)} - \arctan\sqrt{Ma^2-1} \tag{19}$$

The continuous series of expansion waves are approximated express as one wave, and the average shock wave angle is

$$\varepsilon = \sin^{-1}\left(\frac{1}{Ma}\right) = \sin^{-1}\left(\frac{2}{Ma_{s1}+Ma_{s2}}\right) \tag{20}$$

The expansion wave intensity is

$$\beta = \frac{\Pi(Ma_{s2})}{\Pi(Ma_{s1})} \tag{21}$$

Aerodynamic parameters before and after expansion wave $\Pi(Ma_{e1})$, $\Pi(Ma_{e2})$ can be obtained by Eq.4.

When $E=(P_b/P^*)_3$, the oblique shock wave intensity for the gas outlet pressure is equal to ejector chamber back pressure, there is no wave behind the nozzle exit, gas pressure and velocity field of the fluid flow from nozzle outlet are gentle, this is the best design.

3. Results and discussion

When designing ejector, the section ratio of nozzle is usually determined according to the expansion ratio under design condition, and when the nozzle structure is fixed, the change of expansion ratio makes the ejector deviate from the optimal working condition and the emergence of the inevitable shock wave. The above subsection is compiled into a calculation program. Steam, ammonia, R22, R290, R134a and R600a are selected as working materials. Their adiabatic indexes at atmospheric pressure are 1.3, 1.316, 1.185, 1.136, 1.12 and 1.105, respectively. The effects of expansion ratio, nozzle cross section ratio, nozzle cone angle and material parameters of shock wave characteristics were investigated.

The ejector in a certain structure (nozzle exit A_1/A_0=9, nozzle cone angle α=9°), the expansion ratio determines the type, position and intensity of mach waves in the nozzle outlet. As shown in Figs.2 and 3, with expansion ratio increased, expansion wave occurs first, shock wave and cross section than is also increasing, With the expansion ratio increases, the expansion wave first appears, and mach wave intensity and wave angle are basically unchanged. When the expansion ratio $E>(P_b/P^*)_1$, oblique shock wave occurs at the nozzle exit first, and the intensity of shock wave and shock wave angle basically remain unchanged too.

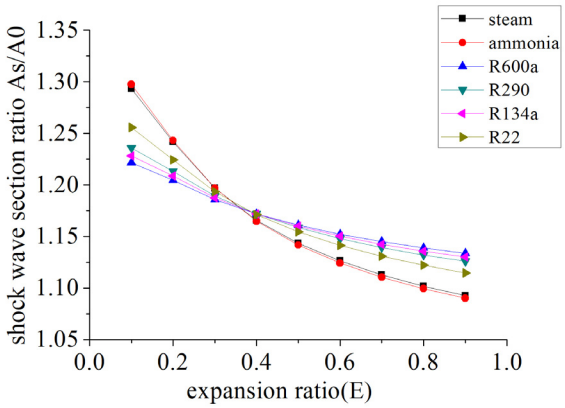

Fig. 2. Influence of expansion ratio on shock wave section ratio.

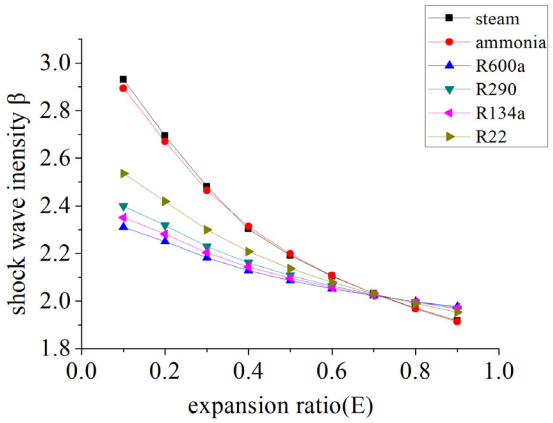

Fig. 3. Influence of expansion ratio on shock wave intensity.

When the expansion ratio $E>(P_b/P^*)_2$, at the nozzle exit appear straight shock, and shock wave section ratio reduces constantly. It shows that the factors influencing the strength of oblique shock wave, expansion wave and shock wave angle are only related to the nozzle structure, not related to the operating conditions of the injector. When the expansion ratio is constant, the cross sections of straight shock wave about ammonia, steam, R22, R290, R134a and R600a increase successively. The strength of positive shock waves decreases successively. The analytic results indicate that shock wave

intensitiy gradient and shock wave section ratio gradient become smaller as the adiabatic index become bigger.

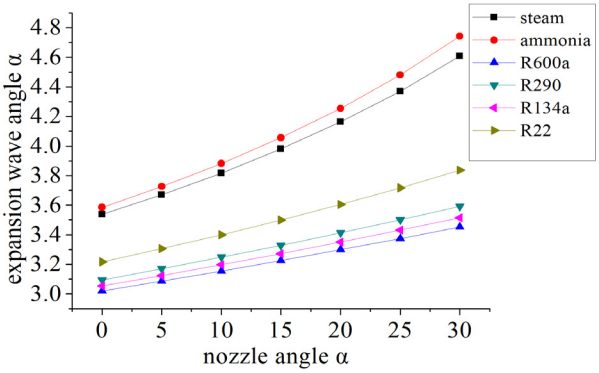

Fig. 4. Influence of nozzle cone angle on expansion wave angle.

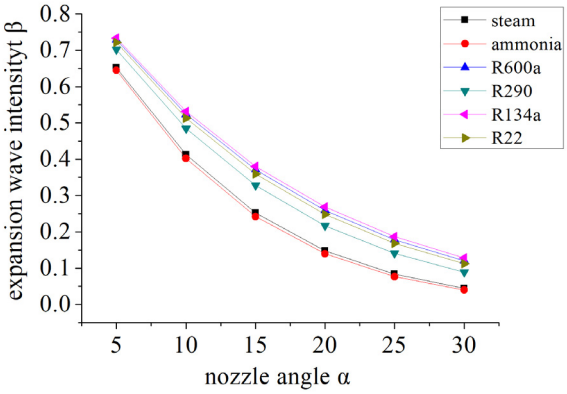

Fig. 5. Influence of nozzle cone angle on expansion wave intensity.

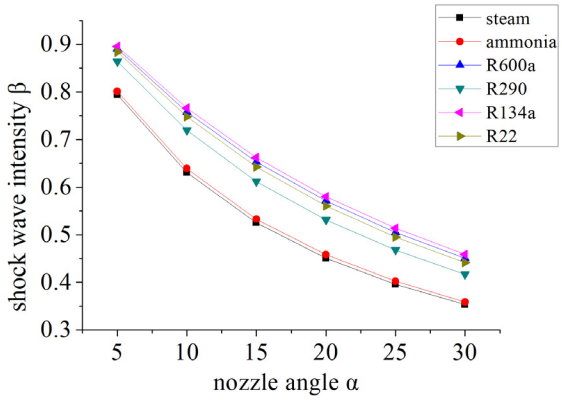

Fig. 6. Influence of nozzle cone angle on shock wave intensity.

At a given expansion ratio and nozzle cone angle (ratio of the nozzle cross section A_1/A_0=9), the influence of nozzle cone angle on shock intensity and shock angle as shown in Figs.4 and 5. The intensity and the angle of shock wave both increased with the increasing of the angle of nozzle. It can be seen that the influence rule of nozzle exit cone angle on the intensity of oblique shock wave and expansion wave is basically the same, and the intensity of shock wave decreases with the increase of nozzle cone angle. The gradient of expansion wave intensity is increasing with nozzle cone angle, and

for different refrigerants, the higher the adiabatic index of the working flow, the higher intensity of expansion wave. In addition, the expansion wave angle and oblique shock wave angle of steam, ammonia, R290 and R600a increased successively. It shows that the adiabatic index of the working flow gets bigger as the expansion wave angle gets smaller.

4. Conclusions

The formation of shock waves inevitably makes the vapor subject to strong shock resistance, the total pressure drops after the refrigerant passes through the shock wave, this situation results in a large irreversible loss. The magnitude of shock resistance depends on the shock intensity, the higher the shock intensity, the greater the shock resistance. Fig. 6 shows normal shock strength greater than the oblique shock wave and expansion wave, so when designing ejector need to satisfy $E=(P_b/P^*)_3$, By this way, only oblique shock waves and expansion waves will appear when the spray is operating at variable operating conditions. When operating conditions make the nozzle outlet appears oblique shock wave (dilatational wave), than the cross section ratio of nozzle and the nozzle cone angle is smaller, the adiabatic index of the working flow higher, the oblique shock wave (dilatational wave) the less strength, and shock resistance. However, the irreversible loss is also related to the friction factor after considering the viscosity of steam, increasing the cross section ratio of nozzle and decreasing the cone angle of nozzle will increase the friction area between steam and wall, and then the irreversible loss caused by friction is increased. Therefore, there should be an optimal parameter interval about the structure design of the actual injector nozzle, so that the efficiency of the nozzle is the highest.

Acknowledgment

The authors acknowledge the financial support by National Natural Science Foundation of China (Grant No. 51366001).

References

[1] J.H. Keenan, E.P. Neumann, F. Lustwerk, An Investigation of Ejector Design By Analysis and Simulation. ASME Journal of Applied Mechanics, **72**(1950): 299-309.

[2] A. Selvaraju, A. Mani, Analysis of an ejector with environment friendly refrigerants[J], Applied Thermal Engineering, **24**(2004): 827–838.

[3] J.M. Abdulateef, K. Sopian, M.A. Alghoul, M.Y. Sulaiman, Review on solar-driven ejector refrigeration technologies, Renewable and Sustainable Energy Reviews, **13**(2009) : 1338–1349.

[4] B.J. Huang, W.Z. Ton, C.C. Wu, H.W. Ko, H.S. Chang, H.Y. Hsu, J.H. Liu, J.H. Wu, R. H. Yen, Performance test of solar-assisted ejector cooling system, International Jounal of Refrigeration, **39** (2014) : 172–185.

[5] V.M. Nguyen, S.B. Riffat, P.S. Doherty, Development of a solar-powered passive ejector cooling system. Applied Thermal Engineering, **21**(2001): 157-168.

[6] J.T. Munday, D.F. Baester, A new ejector theory applied to steam jet refrigeration. Industrial & Engingeering Chemistry Process Design and Development, **16**(1997): 7442-449.

[7] Z. Chen, C. Dang, E. Hihara, Investigations on driving flow expansion characteristics inside ejectors[J]. International Journal of Heat & Mass Transfer, **108**(2017):490-500.